Mg-Cr Layered Double Hydroxide with Intercalated Oxalic Anion for Removal Cationic Dyes Rhodamine B and Methylene Blue

Arini Fousty Badri[1], Neza Rahayu Palapa[1], Risfidian Mohadi[2], Mardiyanto[3], Aldes Lesbani[1*]

[1]Department of Chemistry, Faculty of Mathematics and Natural Sciences, Sriwijaya University, Jl. Palembang-Prabumulih, Km. 32, Ogan Ilir, South Sumatra, Indonesia
[2]Department of Environmental Science, Graduate School, Sriwijaya University, Jl. Padang Selasa No. 524 Ilir Barat 1, Palembang-South Sumatra, Indonesia
[3]Department of Pharmacy, Faculty of Mathematics and Natural Sciences, Sriwijaya University, Jl. Jl. Palembang-Prabumulih, Km. 32, Ogan Ilir 30662, South Sumatra, Indonesia

Abstract

A MgCr-based layered double hydroxide (LDH) was synthesized by a coprecipitation method, followed by an intercalation process using an oxalic anion. The materials were characterized using X-ray diffraction analysis, FT-IR spectroscopy, and pH pzc measurement. The materials were then applied as adsorbents for removal of methylene blue (MB) and rhodamine B (RhB) from aqueous solution. Pristine Mg/Cr LDH exhibited RhB adsorption capacity of 32.154 mg g^{-1}, whereas the use of intercalated Mg/Cr LDH caused an increase in the capacity (139.526 mg g^{-1}). Kinetic studies indicated that the dye adsorption using both LDHs followed a pseudo-second-order kinetic model; the K_2 values of pristine and modified Mg/Cr LDH for RhB and MB were 6.970, 0.001, 0.426, and 2.056 g mg^{-1} min^{-1}, respectively. The thermodynamic study identified that the adsorption of both dyes onto the LDHs was a spontaneous process and can be classified as physical adsorption with adsorption energies of <40 kJ/mol. Moreover, the desorption and regeneration experiments indicated the high economic feasibility and reusability of the LDHs. By using HCl as the optimal solvent, the LDHs could desorb as much as 98% of the dye and could be used as adsorbents with high adsorption capacity over three cycles.

Keywords: Layered double hydroxide, MgCr, rhodamine B, methylene blue, intercalation

1 Introduction

The contamination of water bodies due to dyes negatively affects the ecological system and human health [1]. Industrial activities such as production of textile, paper, and rubber use reactive synthetic dyes [2,3]. Such dyes are harmful organic pollutants because of their carcinogenic effects [3–5]. Dye contaminants are synthetic dyes that are non-biodegradable; therefore, it is recommended to remove such pollutants from wastewater before being discharged into natural water [6]. Several methods have been employed to remove dyes from wastewater, such as ion exchange, filtration, membrane separation, electrochemical degradation, and adsorption methods. Among these methods, adsorption is a suitable method to remove dyes from wastewater because of its low cost and high efficiency and because it involves a simple treatment. Moreover, adsorption efficiency depends on the adsorbent [7,8].

Various adsorbents have been used to remove dyes from wastewater such as bentonite [9], kaoline, activated carbon, zeolites, and hydrotalcite [10–12]. Hydrotalcite is a class of clay materials and serves as effective sorbents [13,14]. However, to achieve high efficiency for dye adsorption, hydrotalcite must be modified using an intercalating process with organic [15] or inorganic anions to increase its surface area [16]. Hydrotalcites have been extensively modified to impart high adsorption capacity and efficiency; such modification methods include development of LDH-MnFe$_2$O$_4$ hybrid materials [17] and intercalation of LDHs with aromatic acid anions [18].

Anionic synthetic clay layered double hydroxides (LDHs) consist of divalent and trivalent brucite-like layers that have a positive charge and an anion functioning as a counterion. These compounds have a general formula of $[M^{II}_{(1-x)} M^{III}_x (OH)_2]^{x+}(An^-)^{x/n} \cdot mH_2O$, where An^- is the intercalated anion [19–21]. The anion in the interlayer of the LDH can be replaced, under suitable conditions, with inorganic ions such as nitrate, carbonate [22], and sulfate ions in order to enhance the interlayer. Modified LDHs have applications in various fields, especially in dye removal. According to Santos *et al.*, calcined LDH was used to adsorb acid yellow 42 in aqueous solutions [23]. Deng *et al.* [24]

Corresponding author: Aldes Lesbani, Department of Chemistry, Faculty of Mathematics and Natural Sciences, Sriwijaya University, Jl. Palembang-Prabumulih, Km. 32, Ogan Ilir, South Sumatra, Indonesia. E-mail: aldeslesbani@pps.unsri.ac.id

reported the use of sodium-dodecyl-sulfate-intercalated and acrylamide-anchored LDH for the removal of Congo red. In contrast, Xu *et al.* prepared polyoxometalate-intercalated ZnAlFe LDH, which exhibited improved adsorption capacity for cationic dye removal [14]. Similarly, Li *et al.* used a magnetic core-shell dodecyl-sulfate-intercalated LDH nanocomposite to adsorb cationic and anionic organic dyes [25].

In this study, Mg/Cr LDH was synthesized by a coprecipitation method. The LDH was modified by intercalating oxalate anions ($C_2O_4^{2-}$) into the interlayer space of hydrotalcite via anion exchange. The pristine and intercalated LDHs were then applied as adsorbents for removal of rhodamine B (RhB) and methylene blue (MB). The structures of these dyes are presented in Fig. 1. The adsorption of the dyes using the intercalated LDH material was then optimized by varying the contact time, initial concentration, and temperature. A desorption process was conducted to determine a suitable solvent using several organic solvents, followed by regeneration over three cycles.
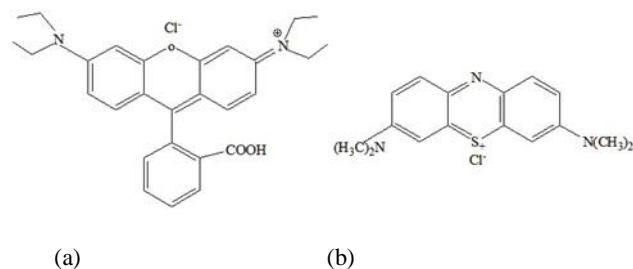

(a)   (b)

Figure 1: Structures of (a) rhodamine B and (b) methylene blue

2 Materials and Methods

The chemicals used in this study were $Mg(NO_3)_2 \cdot 6H_2O$ (Sigma-Aldrich, 400.15 g/mol), $Cr(NO_3)_3 \cdot 9H_2O$ (EMSURE® ACS, Reag. Ph Eur, 256.41 g/mol), Na_2CO_3 (EMSURE® ACS, Reag. Ph Eur, 126.07 g/mol), NaOH (EMSURE® ACS, Reag. Ph Eur, 40 g/mol), HCl (MallinckrodtAR®, 37%), and $H_2C_2O_4 \cdot 2H_2O$ (EMSURE® ACS, Reag. Ph Eur, 126.07 g/mol). All chemicals were used as received without further purification. X-ray diffraction (XRD) analysis was performed using a Rigaku Miniflex-6000 diffractometer, and the sample was scanned at 10°/min The Brunauer–Emmett–Teller (BET) surface area was measured using a Quantachrome adsorption–desorption apparatus. The sample was degassed prior to analysis at 77 K. Fourier transform infrared (FT-IR) spectroscopy was performed using a Shimadzu Prestige-21 device, with the use of KBr pellets; each sample was analyzed at wavenumbers in the range of 400–4000 cm^{-1}. The concentrations of the dyes were measured using a Biobase BK 1800 UV-Visible spectrophotometer.

2.1 Synthesis Mg/Cr LDH

Mg/Cr LDH was synthesized by a coprecipitation method. First, a solution of $Mg(NO_3)_2 \cdot 6H_2O$ was mixed with $Cr(NO_3)_3 \cdot 9H_2O$ (3:1) and stirred for 30 min. A solution of Na_2CO_3 (1 M) and NaOH (2 M) was added to the reaction mixture. The mixture was then mixed under continuous stirring until a precipitate was formed, and then the pH of the solution was adjusted to 10 using NaOH. The reaction was maintained at 80 °C

for 24 h to produce Mg/Cr LDH. The solid material was then heated at 80 °C for 24 h.

2.2 Intercalation of Mg/Cr LDH with Oxalic Anion

Mg/Cr LDH intercalated with oxalic anions was prepared by the ion-exchange method. As much as 50 g of Mg/Cr LDH was mixed with water, and the solution was stirred for 60 min under a nitrogen atmosphere. The LDH mixture was then added to a solution of oxalic acid. The pH of the mixture was adjusted to 9 using NaOH. The suspension was stirred for 24 h under a N_2 atmosphere and dried at 100 °C.

2.3 Adsorption of Methylene Blue and Rhodamine B using Mg/Cr LDH and Intercalated Mg/Cr LDH

First, 0.02 g of LDH was added to 20 mL of MB and RhB, each having a concentration of 70 mg/L. The adsorption studies were carried out under stirring over different durations (5–120 min). After stirring, the suspensions were separated by centrifugation at 3000 rpm for 10 min and examined via UV-Vis spectrophotometry at 662 nm for methylene blue and 555 nm for rhodamine B. After equilibrium was reached, 0.5 g of LDH was used to adsorb the dyes at different dye concentrations (10–60 mg/L) and temperatures (303–333 K).

2.4 Desorption and Regeneration of Methylene Blue and Rhodamine B using Mg/Cr LDH and Intercalated Mg/Cr LDH

A desorption process was performed to examine the efficiency of the adsorbent. First, 0.5 g of LDH was added to 50 mL of MB and RhB (100 ppm) and shaken for 120 min. Then, the dye concentration in the filtrate was determined by UV-Vis spectrophotometry, followed by drying of the adsorbent for 2 h. The residue (0.01 g) was shaken in 10 mL solvent (HCl, NaOH, hydroxylamine hydrochloride, water, and Na-EDTA) for 120 min. The filtrate was examined via UV-Vis spectrophotometry. The regeneration process was carried out using three cycles of the adsorption–desorption process.

3 Results and Discussion

The diffraction patterns of the pristine and modified Mg/Cr LDHs are shown in Fig. 2. The diffractogram of the pristine Mg/Cr LDH (Fig. 2a) consisted of both sharp and symmetrical peaks and some high-intensity asymmetrical peaks. This result explains the highly crystalline and ordered layered structure of Mg/Cr LDH. The typical pattern corresponding to hydrotalcite is evident, which is a set of four reflection lines at $2\theta = 11°$, $22°$, $36°$, and $60°$ that are ascribed to the reflections of the (003), (006), (115), and (110) basal planes, respectively. The interlayer distance of the pristine LDH was 7.62 Å (Fig. 2a). The XRD pattern of Mg/Cr-oxalate LDH exhibits a lower intensity than that before intercalation, indicating a decrease in the crystallinity of the LDH interlayer due to the presence of oxalate (Fig. 2b). The (003) reflection suggests that the reflection shifted to lower angles which indicated an increase in the basal spacing of Mg/Cr-oxalate LDH (11.35 Å). The peak shift from $2\theta = 11°$ to $10°$ indicates the replacement of nitrate ions with oxalate ions in the interlayer. Hence, the intercalation process with the oxalate anion was successful, and significant interlayer separation was achieved.
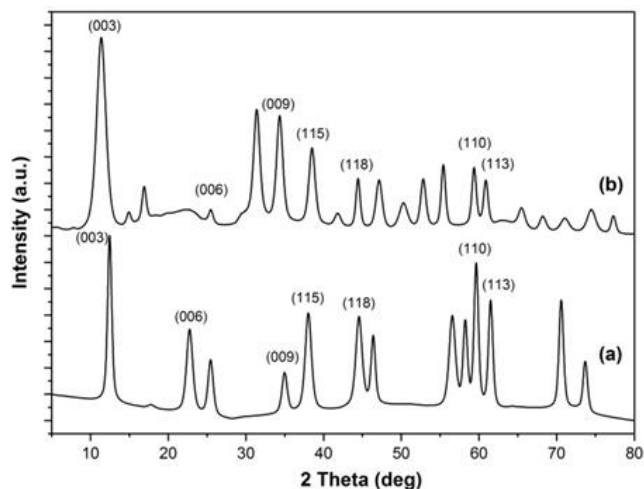
Figure 2: X-ray Powder diffraction patterns of Mg/Cr LDH (a) and intercalated Mg/Cr LDH(b)

Figs. 3a and b show the graphs of the BET curves of Mg/Cr LDH and intercalated Mg/Cr LDH; these graphs indicated that both materials followed type IV isotherm patterns according to IUPAC classifications and that the materials were mesoporous; occurrence of hysteresis was also confirmed. The materials Mg/Cr and intercalated Mg/Cr LDH contained mesopores that were 2–50 nm in size, based on IUPAC classifications. The isotherms of both Mg/Cr LDH and intercalated Mg/Cr LDH were ascribed to type H2 because the material contained large mesopores [26]. Table 1 summarizes the surface areas and pore sizes of Mg/Cr LDH and intercalated Mg/Cr LDH. The results indicated an increase in the surface area by as much as 26.1153 m^2/g after intercalation, which resulted in a decrease in the pore diameter of the LDH.
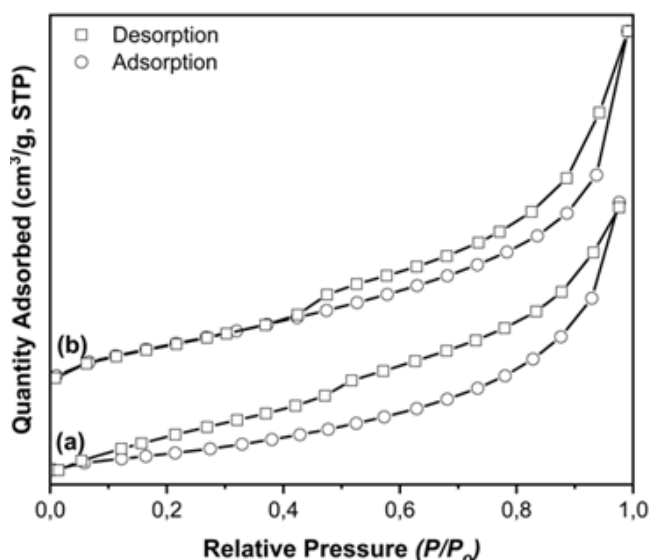

Figure 3: N$_2$ Adsorption–desorption of Mg/Cr LDH (a) and intercalated Mg/Cr LDH (b)
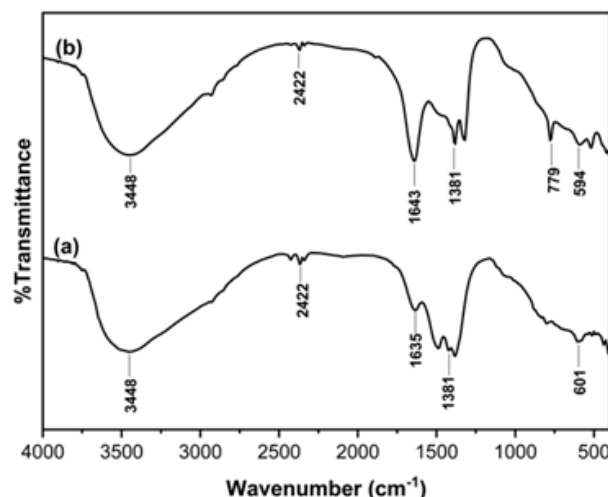

Figure 4: FT-IR spectra of Mg/Cr LDH (a) and intercalated Mg/Cr LDH (b)

Fig. 4 presents the FT-IR spectra of the materials. All samples exhibited broad bands at around 3400 cm^{-1}, indicating the presence of an OH group. This band may be attributed to the hydroxyl group of water molecules, and the interlayer anions could also account for the broadening of this band. The bending mode of water gave rise to a rather weak band around 1635 cm^{-1} in the FT-IR spectra of Mg/Cr LDH (Fig. 4a). The vibrational modes of the interlayer nitrate ions are indicated by the peak at 1381 cm^{-1}. This spectrum is observed for every hydroxide irrespective of nature. The octahedral sheets suggest a rather symmetric environment for the interlayer anions. The absorption peaks below 1000 cm^{-1} correspond to M-O and M-O-M vibrations. The presence of oxalate anions in the LDH was confirmed by the presence of a peak at 1381 cm^{-1} (Fig. 4b), which could be assigned to the stretching modes of the carboxylate group.

Furthermore, the relatively weak peaks at 779 and 594 cm^{-1} correspond to the carbon-oxygen bond in the carboxyl group [27]. In addition, the strong absorption peak of the nitrate anions in Fig. 4a decreased after the ion-exchange reaction (Fig. 4b). This result indicated that oxalate anions replaced the interlamellar nitrate anions, as previously evidenced by X-ray analysis.

The stabilities of the pristine and modified LDHs were determined by pH point zero charges (pzc), as shown in Fig. 5. The pristine and modified LDHs prior to use as dye adsorbents were examined using pH pzc to determine the charge of the materials. As shown in Fig. 5, the cross point was identified at pH 9 for both pristine and modified LDHs. A pH of 9 was ascribed to the material when it has no charge. As such, the materials have positive charges below pH 9 and negative charges above pH 9.
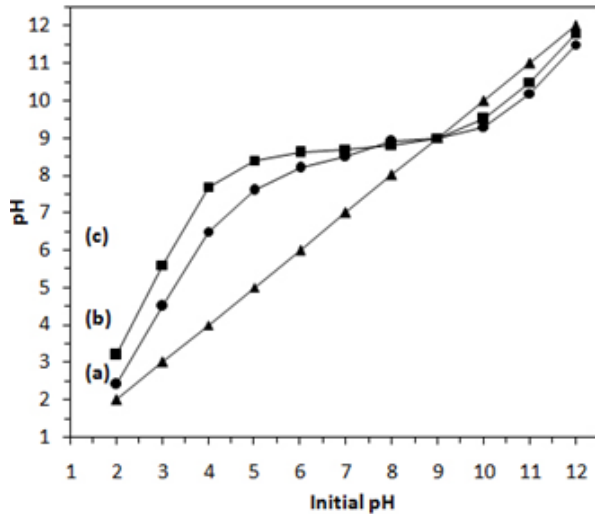
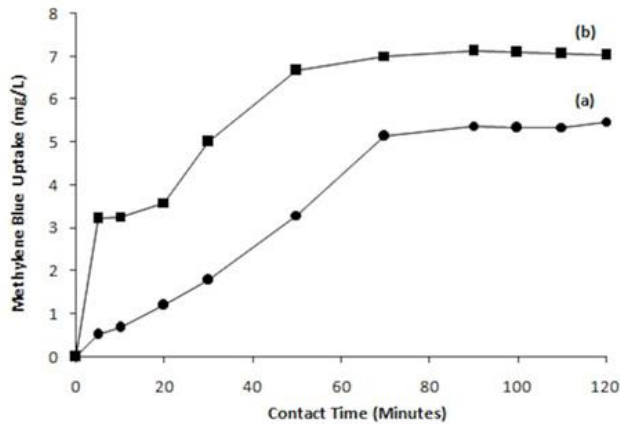Figure 5: pH pzc graphs of Mg/Cr LDH (a) and intercalated Mg/Cr LDH (b)

Figure 6: Time variation of adsorption of methylene blue on Mg/Cr LDH (a) and intercalated Mg/Cr LDH (b)

The results of the adsorption of MB by MgCr LDH and MgCrC$_2$O$_4^-$ LDH, which was conducted at pH 9, are shown in Fig. 6. The adsorption equilibrium was reached after 70 min with a MB uptake of 4.9 mg/L for pristine LDH and 6.5 mg/L for the modified LDH. This contact time was considered optimal for the next experiment. The adsorption of RhB using modified LDH, as shown in Fig. 7, improved slightly and reached equilibrium after

70 min; equilibrium was reached after 20 min for pristine LDH. The RhB uptake using the modified Mg/Cr LDH was twice that of pristine Mg/Cr LDH, with each adsorbing 43 mg/L and 19 mg/L of RhB, respectively.
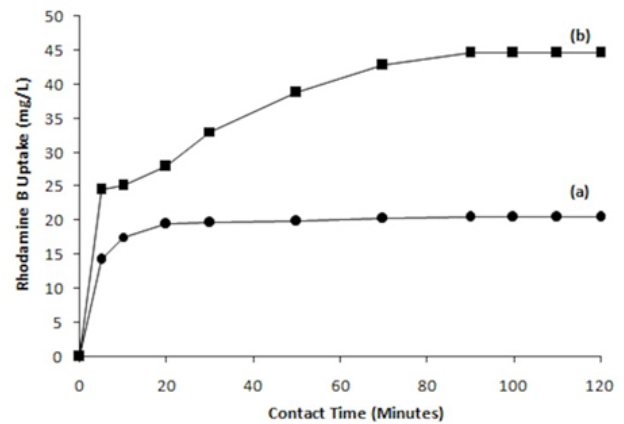

Figure 7: Time variation adsorption of rhodamine B on Mg/Cr LDH (a) and intercalated Mg/Cr LDH (b)

The effect of contact time on the adsorption of dyes on pristine and modified Mg/Cr LDHs was shown in Fig. 8. The amount of dye adsorbed by LDHs notably increased with increasing contact time. However, the sorption rate of the dyes on the pristine LDH was slightly lower than that on the modified LDH. The kinetics results indicate that the modified LDH exhibited a higher sorption efficiency for both dyes. Pseudo-first-order and pseudo-second-order kinetic models were applied to determine the kinetic sorption process; such models are respectively expressed as follows:

$$\ln (q_e - q_t) = \ln q_e - k_1 t \tag{1}$$

$$t/q_t = 1/(k_2 q_e^2) + (1/q_e)\, t, \tag{2}$$

where q_t (mg/g) is the concentration of dye adsorbed at time t (min), q_e (mg/g) is the concentration of dye adsorbed at equilibrium, k_1 is the rate constant of first-order sorption, and k_2 is the rate constant of pseudo-second-order (PSO) sorption. The results of such calculations are shown in Table 2. This table shows that the sorption of the dyes on pristine LDH and modified LDH conform to the PSO kinetic model. The results suggest that interactions between the sorbate and sorbent were presented.

Table 2: Kinetic parameters of dyes adsorption onto Mg/Cr-LDH and intercalated Mg/Cr LDH

LDH		PFO				PSO		
		Co (mg/L)	qe (mg/g)	K_1 (min^{-1})	R^2	qe(mg/g)	K_2(g mg min^{-1})	R^2
Mg/Cr	Rh-B	50	41.572	0.003	0.801	0.409	6.970	0.9878
Mg/Cr-oxalate	Rh-B	50	47.022	0.056	0.897	2.350	0.426	0.988
Mg/Cr	MB	10	7.786	0.040	0.935	10.225	0.001	0.940
Mg/Cr-oxalate	MB	10	10.022	0.081	0.904	0.486	2.056	0.992

The data on the effect of dye concentration and temperature, as shown in Figs. 8 and 9. It can be observed that increasing the concentration and temperature would increase the amount of dye adsorbed on both pristine and modified LDHs. There is a specific increase in the concentration of adsorbed RhB at 30 mg/L (Fig. 8a), which is probably due to the physical adsorption of RhB as the interaction between the sorbate and sorbent was at equilibrium. The increasing trend for the adsorption isotherm of RhB on modified LDH was determined from the data in Fig. 8a using Langmuir and Freundlich equations. Fig. 8b exhibits a similar behavior for the adsorption of RhB, which was at a concentration of 15 mg/L, as observed for the curves with increasing temperature.
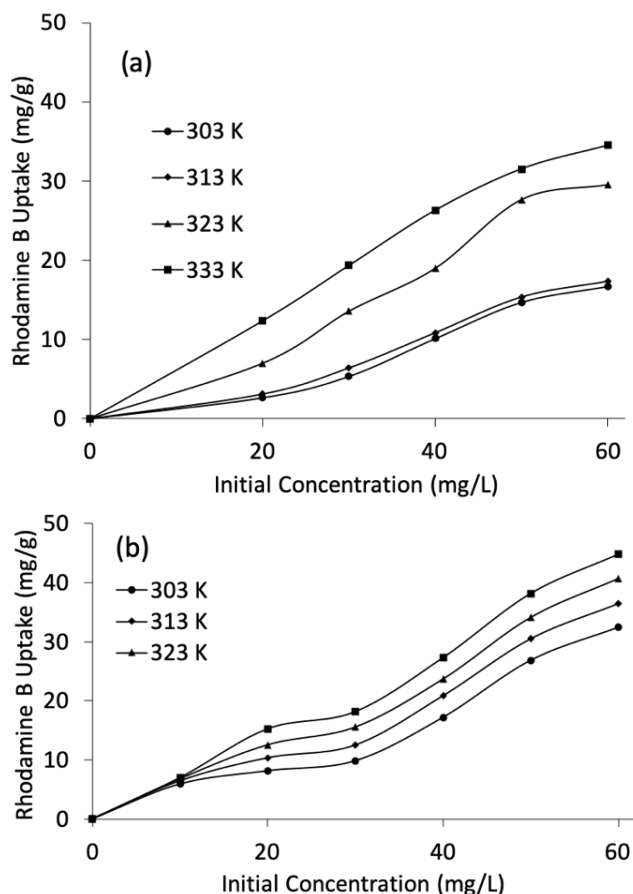

Figure 8: RhB uptake by initial concentration at various temperatures by Mg/Cr LDH (a) and intercalated Mg/Cr LDH (b)

The results of the adsorption of MB onto pristine LDH and modified LDH are shown in Fig. 9. For the adsorption of MB on both adsorbents, the difference in dye uptake at different temperatures was not significant. As shown in Fig. 9a, the adsorption rate of MB on pristine LDH was 23 mg/g at 333 K, which indicated a higher adsorption capacity. Tables 3 and 4 summarize the isotherm parameters for the adsorption of the dyes on pristine LDH and modified LDH. The adsorption isotherm data for RhB is shown in Table 5 The data indicated that the isotherm was best represented by the Freundlich isotherm.
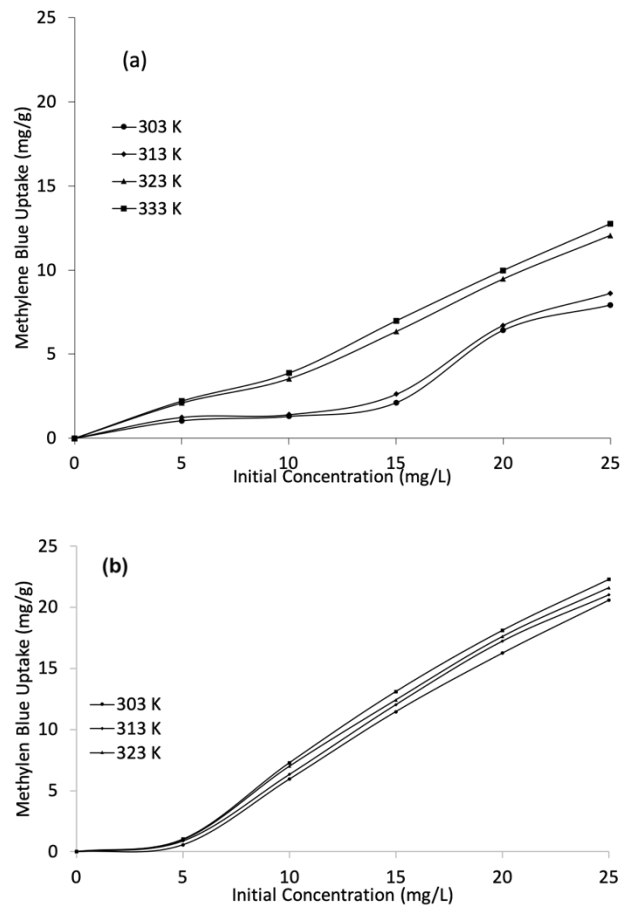

Figure 9: MB uptake by initial concentration at several temperatures by Mg/Cr LDH (a) and intercalated Mg/Cr LDH (b)

The Freundlich isotherm indicates a multilayer adsorption process. Based on the adsorption capacity of RhB on pristine and modified Mg/Cr LDHs, an increase in temperature is correlated with increasing adsorption capacity at equilibrium, as summarized in Table 3. The adsorption data of MB on pristine and modified Mg/Cr LDH is summarized in Table 4. The data indicates that the adsorption using pristine and modified Mg/Cr LDHs was best represented by the Freundlich isotherm. The increase in temperature caused the adsorption capacity to be higher at 333 K than at room temperature. The maximum adsorption capacities for both dyes using modified Mg/Cr LDH were higher than those using pristine Mg/Cr LDH. According to Leon et al. [28], the higher content of available carboxylic groups promotes electrostatic interactions between the sorbate and sorbent. The amount of dye adsorbed as a function of temperature is summarized in Tables 5 and 6. The data in Tables 5 and 6 indicate increasing adsorption capacity with increasing temperature in the range of 303–333 K.

Table 3: Isotherms parameter of adsorption rhodamine B onto Mg/Cr-LDH and intercalated Mg/Cr LDH

LDH	adsorption isotherm	adsorption constant	T(K)			
			303	313	323	333
Mg/Cr	Langmuir	Q_{max}	20.960	27.855	28.011	32.154
		K_L	0.023	0.03	0.034	0.032
		R^2	0.723	0.637	0.684	0.665
	Freundlich	N	0.744	0.75	0.642	0.67
		K_F	1.909	1.758	2.279	1.866
		R^2	0.947	0.866	0.914	0.896
Mg/Cr - Oxalate	Langmuir	Q_{max}	74.828	77.778	120.482	139.526
		K_L	0.003	0.004	0.010	0.029
		R^2	0.020	0.067	0.135	0.659
	Freundlich	N	1.039	0.945	0.900	0.661
		K_F	1.109	1.106	1.084	1.691
		R^2	0.930	0.962	0.912	0.913

Table 4: Isotherms parameter of adsorption methylene blue onto Mg/Cr-LDH and intercalated Mg/Cr LDH

LDH	adsorption isotherm	adsorption constant	T(K)			
			303	313	323	333
Mg/Cr	Langmuir	Q_{max}	1.636	1.517	1.452	1.538
		K_L	1.323	5.131	1.534	1.195
		R^2	0.926	0.955	0.938	0.964
	Freundlich	N	0.446	0.497	0.572	0.629
		K_F	2.912	1.625	1.142	2.160
		R^2	0.991	0.993	0.981	0.980
Mg/Cr – Oxalate	Langmuir	Q_{max}	8.741	4.854	2.879	2.625
		K_L	0.107	0.934	0.771	0.851
		R^2	0.814	0.918	0.902	0.784
	Freundlich	N	0.501	0.630	0.644	0.562
		K_F	1.957	7.638	7.132	2.160
		R^2	0.961	0.938	0.877	0.981

Table 5: Thermodynamic adsorption parameter of rhodamine B onto Mg/Cr-LDH and intercalated Mg/Cr LDH

T (K)	C	ΔH (kJ/mol)	ΔS (kJ/mol)	ΔG (kJ/mol)	ΔH (kJ/mol)	ΔS (kJ/mol)	ΔG (kJ/mol)
303				-0.362			0.812
313	40 mg/L	24.160	0.081	-1.171	27.883	0.089	-0.081
323				-1.981			-0.975
333				-2.790			-1.868
303				-1.255			-0.180
313	50 mg/L	8.681	0.033	-1.582	26.981	0.090	-1.076
323				-1.910			-1.973
333				-2.238			-2.869
303				-1.350			-0.229
313	60 mg/L	14.584	0.053	-1.876	24.437	0.081	-1.043
323				-2.401			-1.857
333				-2.927			-2.671

The adsorption process was described by thermodynamic parameters such as Gibbs free energy, enthalpy, and entropy, which can be expressed in a single equation as follows:

$$\Delta G = \Delta H - T\Delta S \qquad (3)$$

where ΔG is the change in Gibbs free energy (kJ/mol), ΔS is the change in entropy (kJ/mol), and ΔH is the change in entropy (kJ/mol). The ΔH and ΔS values were determined from the y-intercept and slope (eq. 3), respectively, as listed in Tables 5 and 6. The ΔS values were positive, which indicated an increase in randomness during the ongoing process. The positive ΔH values indicated that the adsorption was endothermic and proceeded via a physisorption process. The likelihood of the adsorption proceeding via a physisorption process was supported by the ΔG values which were within the range of −20–0 kJ/mol. The negative Gibbs free energy values indicate that the adsorption was

spontaneous. In addition, the ΔH values calculated in this study (−20 kJ/mol) are consistent with the hydrogen bond and dipole bond forces of the adsorbent. The adsorption capacities for MB

and RhB in this study are comparable to those of other adsorbents reported in previous literature, which are listed in Table 7.

Table 6: Thermodynamic adsorption parameter of methylene blue onto Mg/Cr-LDH and intercalated Mg/Cr LDH

T (K)	C	ΔH (kJ/mol)	ΔS (kJ/mol)	ΔG (kJ/mol)	ΔH (kJ/mol)	ΔS (J/Kmol)	ΔG (kJ/mol)
303			0.031	-2.145			-2.972
313	20 mg/L	7.198		-2.453	15.070	0.060	-3.568
323				-2.761			-4.163
333				-3.070			-4.758
303				-2.581			-3.209
313	25 mg/L	22.114	0.081	-3.396	12.311	0.051	-3.722
323				-4.211			-4.234
333				-5.026			-4.746
303				-3.871			-2.840
313	30 mg/L	5.682	0.032	-4.187	7.431	0.034	-3.179
323				-4.502			-3.518
333				-4.817			-3.857

Table 7: Comparison of adsorption capacity of some adsorbents for RhB and MB removal

Dyes	Adsorbent	Adsorption Capacity (mg/g)	References
MB	Ti-Al-Si-O	162.96	(29)
RhB	Nanocomposite Adsorbent	142.8	(30)
MB	Nanocomposite SNF/MNP/PS	103.1	(31)
RhB	Casuarina Equisetifolia Needle (CEN)	82.34	(32)
RhB	Activated Cotton Stalks (CSAC)	133.33	(33)
MB		153.85	
RhB	Magnetic Lignosulfonate (MLS)	22.47	(34)
RhB	Magnetic AC/CeO$_2$	324.6	(35)
RhB	Boron Organic Polymers	1,388	
RhB	Chitosan graft poly	556.9	(36)
MB		936	
RhB	SA/HEC/HA Membrane	18.814	(37)
MB		20.83	
MB	Nanocomposite hydrogel	122.5	(38)
RhB		62	
RhB	MgCr	32.154	This work
Mb		1.636	This work
RhB	Intercalated MgCr	139.526	This work
MB		8.741	This work
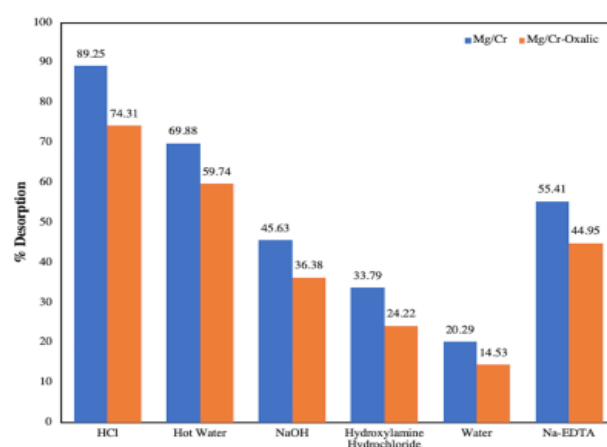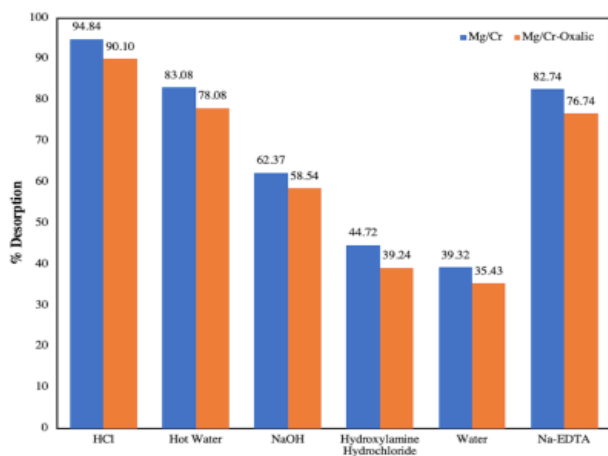
(a)   (b)

Figure. 10: Desorption of RhB (a) and MB (b) on Mg/Cr-LDH and on intercalated Mg/Cr LDH
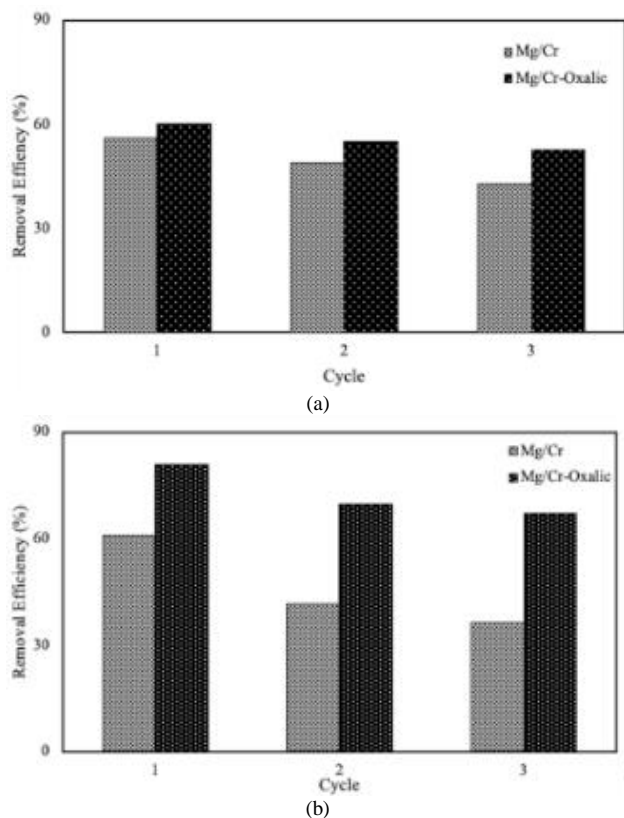
(a)

(b)

Figure. 11: Regeneration of RhB (a) and MB (b) on MgCr LDH and on intercalated Mg/Cr LDH

The desorption study was conducted in several solvents onto MgCr and MgCr modified. Figure 10 shows the y axis is percent desorption using RhB onto MgCr and MgCr modified. As our best acknowledgment, a few the researchers have focused to recovery used material. Several solvent organic, acid, and base were conducted in this treatment for suitable solvents (ie, water, HCl, NaOH, $HONH_3Cl$ and Na-EDTA). The result on Figure 10 shows that the higher desorption is HCl. In this case, MgCr modified has lower desorption than MgCr pristine. we assumed that the dye is more trapped in the active site of adsorbents and requires a long time to be desorbed. On the other hand, in acid solution, the hydrotalcite pristine is more desorbed than modified caused the hydrotalcite can be exfoliated (Palapa et al. 2020). The regeneration of MgCr LDH and intercalated MgCr LDH was investigated by three times cycles. The recycling process of LDHs adsorption-desorption was illustrated in Figure 11. The high effectivity of reuse material showed after intercalated with oxalic anions than pristine. These phenomena caused that LDH pristine can be broken in the acid solution for extended uses. The decreases in removal efficiency from LDH pristine indicated that the structure of LDH is exfoliated and ruined.

4 Conclusion

MgCr and MgCr intercalated anion oxalate were easily prepared by the ion-exchange method. MgCr modified anion oxalate has higher adsorbed capacity in equilibrium than pristine amount MgCr modified anion oxalic has higher adsorption

capacity than pristine LDH amount from 32.154 mg.g^{-1} for pristine LDH and 139.526 mg.g^{-1} for intercalated MgCr LDH in RhB dye. The adsorption of both sorbents for MB and RhB was classified as physical adsorption with ΔH^o value in the range under 40 kJ/mol. Moreover, both adsorbents can be reused for further adsorption process. This result based on the desorption results that the RhB and MB can be desorbed from the adsorbent as much as 98%.

Competing interests

The authors declare that there is no conflict of interest that would prejudice the impartiality of this scientific work.

Authors' contribution

All authors of this study have a complete contribution for data collection, data analyses and manuscript writing

References

1. F. Zhang, X. Tang, Y. Huang, A. A. Keller and J. Lan, Competitive removal of Pb2+ and malachite green from water by magnetic phosphate nanocomposites, *Water Res.* (2019) 442–451.
2. E. H. Elkhattabi, M. Lakraimi, M. Berraho, A. Legrouri, R. Hammal and L. El Gaini, Acid Green 1 removal from wastewater by layered double hydroxides, *Appl. Water Sci.* **8** (2018) 1–11.
3. F. A. Dawodu, C. U. Onuh, K. G. Akpomie and E. I. Unuabonah, Synthesis of silver nanoparticle from Vigna unguiculata stem as adsorbent for malachite green in a batch system, *SN Appl. Sci.* **1** (2019) 1–10.
4. Q. Zhang, Q. Lin, X. Zhang and Y. Chen, A novel hierarchical stiff carbon foam with graphene-like nanosheet surface as the desired adsorbent for malachite green removal from wastewater, *Environ. Res.* **179** (2019) 108746.
5. S. Boubakri, M. A. Djebbi, Z. Bouaziz, P. Namour, N. Jaffrezic-Renault, A. B. H. Amara, M. Trabelsi-Ayadi, I. Ghorbel-Abid and R. Kalfat, Removal of two anionic reactive textile dyes by adsorption into MgAl-layered double hydroxide in aqueous solutions, *Environ. Sci. Pollut. Res.* **25** (2018) 23817–23832.
6. Y. Lu, B. Jiang, L. Fang, F. Ling, J. Gao, F. Wu and X. Zhang, High performance NiFe layered double hydroxide for methyl orange dye and Cr(VI) adsorption, *Chemosphere* **152** (2016) 415–422.
7. F. Mohamed, M. R. Abukhadra and M. Shaban, Removal of safranin dye from water using polypyrrole nanofiber/Zn-Fe layered double hydroxide nanocomposite (Ppy NF/Zn-Fe LDH) of enhanced adsorption and photocatalytic properties, *Sci. Total Environ.* **640–641** (2018) 352–363.
8. S. Mallakpour and M. Hatami, An effective, low-cost and recyclable bio-adsorbent having amino acid intercalated LDH@Fe3O4/PVA magnetic nanocomposites for removal of methyl orange from aqueous solution, *Appl. Clay Sci.* **174** (2019) 127–137.
9. T. Taher, D. Rohendi, R. Mohadi and A. Lesbani, Thermal Activated of Indonesian Bentonite as A Low-Cost Adsorbent for Procion Red Removal from Aqueous Solution, *J. Pure Appl. Chem. Res.* **7** (2018) 79–93.
10. H. Zhou, Z. Jiang and S. Wei, A new hydrotalcite-like absorbent FeMnMg-LDH and its adsorption capacity for Pb2 + ions in water, *Appl. Clay Sci.* **153** (2018) 29–37.
11. I. Harizi, D. Chebli, A. Bouguettoucha, S. Rohani and A. Amrane, A New Mg–Al–Cu–Fe-LDH Composite to Enhance the Adsorption of

Acid Red 66 Dye: Characterization, Kinetics and Isotherm Analysis, *Arab. J. Sci. Eng.* **44** (2019) 5245–5261.

12. K. Abdellaoui, I. Pavlovic, M. Bouhent, A. Benhamou and C. Barriga, A comparative study of the amaranth azo dye adsorption/desorption from aqueous solutions by layered double hydroxides, *Appl. Clay Sci.* **143** (2017) 142–150.

13. S. Yanming, L. Dongbin, L. Shifeng, F. Lihui, C. Shuai and M. A. Haque, Removal of lead from aqueous solution on glutamate intercalated layered double hydroxide, *Arab. J. Chem.* **10** (2017) S2295–S2301.

14. M. Xu, B. Bi, B. Xu, Z. Sun and L. Xu, Polyoxometalate-intercalated ZnAlFe-layered double hydroxides for adsorbing removal and photocatalytic degradation of cationic dye, *Appl. Clay Sci.* **157** (2018) 86–91.

15. T. Kameda, H. Takeuchi and T. Yoshioka, NiAl layered double hydroxides modified with citrate, malate, and tartrate: Preparation by coprecipitation and uptake of Cu 2 from aqueous solution, *J. Phys. Chem. Solids* **72** (2011) 846–851.

16. A. Lesbani, D. R. Maretha, T. Taher, Miksusanti, R. Mohadi and R. Andreas, Layered double hydroxides Mg/Fe intercalated H3[α-PW12O40]· n H2O as adsorbent of cadmium(II), *AIP Conf. Proc.* **2049** (2018).

17. O. Mrózek, P. Ecorchard, P. Vomáčka, J. Ederer, D. Smržová, M. Š. Slušná, A. Machálková, M. Nevoralová and H. Beneš, Mg-Al-La LDH-MnFe2O4 hybrid material for facile removal of anionic dyes from aqueous solutions, *Appl. Clay Sci.* **169** (2019) 1–9.

18. S. Yu, X. Wang, Z. Chen, J. Wang, S. Wang, T. Hayat and X. Wang, Layered double hydroxide intercalated with aromatic acid anions for the efficient capture of aniline from aqueous solution, *J. Hazard. Mater.* **321** (2017) 111–120.

19. N. R. Palapa, Y. Saria, T. Taher, R. Mohadi and A. Lesbani, Synthesis and Characterization of Zn/Al, Zn/Fe, and Zn/Cr Layered Double Hydroxides: Effect of M3+ ions Toward Layer Formation, *Sci. Technol. Indones.* **4** (2019) 36–39.

20. H. Starukh and S. Levytska, The simultaneous anionic and cationic dyes removal with Zn–Al layered double hydroxides, *Appl. Clay Sci.* **180** (2019) 0–5.

21. M. Shafigh, M. Hamidpour and G. Furrer, Zinc release from Zn-Mg-Fe(III)-LDH intercalated with nitrate, phosphate and carbonate: The effects of low molecular weight organic acids, *Appl. Clay Sci.* **170** (2019) 135–142.

22. M. N. Sepehr, T. J. Al-Musawi, E. Ghahramani, H. Kazemian and M. Zarrabi, Adsorption Performance of Magnesium/Aluminum Layered Double Hydroxide Nanoparticles for Metronidazole From Aqueous Solution, *Arab. J. Chem.* **10** (2017) 611–623.

23. R. M. M. dos Santos, R. G. L. Gonçalves, V. R. L. Constantino, C. V. Santilli, P. D. Borges, J. Tronto and F. G. Pinto, Adsorption of Acid Yellow 42 dye on calcined layered double hydroxide: Effect of time, concentration, pH and temperature, *Appl. Clay Sci.* **140** (2017) 132–139.

24. L. Deng, H. Zeng, Z. Shi, W. Zhang and J. Luo, Sodium dodecyl sulfate intercalated and acrylamide anchored layered double hydroxides: A multifunctional adsorbent for highly efficient removal of Congo red, *J. Colloid Interface Sci.* **521** (2018) 172–182.

25. Y. Li, H. Y. Bi, Y. Q. Liang, X. M. Mao and H. Li, A magnetic core-shell dodecyl sulfate intercalated layered double hydroxide nanocomposite for the adsorption of cationic and anionic organic dyes, *Appl. Clay Sci.* **183** (2019) 105309.

26. M. Oktriyanti, N. R. Palapa, R. Mohadi and A. Lesbani, Indonesian Journal of Environmental Management and Sustainability Modification Of Zn-Cr Layered Double Hydroxide With Keggin Ion, *Indones. J. Environ. Manag. Sustain.* **3** (2019) 93–99.

27. E. Coronado, C. Martí-Gastaldo, E. Navarro-Moratalla and A. Ribera, Intercalation of [M(ox)3]3- (M = Cr, Rh) complexes into NiIIIFeIII-LDH, *Appl. Clay Sci.* **48** (2010) 228–234.

28. O. León, A. Muñoz-Bonilla, D. Soto, D. Pérez, M. Rangel, M. Colina and M. Fernández-García, Removal of anionic and cationic dyes with bioadsorbent oxidized chitosans, *Carbohydr. Polym.* **194** (2018) 375–383.

29. U. Pal, A. Sandoval, S. I. U. Madrid, G. Corro, V. Sharma and P. Mohanty, Mixed titanium, silicon, and aluminum oxide nanostructures as novel adsorbent for removal of rhodamine 6G and methylene blue as cationic dyes from aqueous solution, *Chemosphere* **163** (2016) 142–152.

30. M. I. Mohammed and S. Baytak, Synthesis of Bentonite–Carbon Nanotube Nanocomposite and Its Adsorption of Rhodamine Dye From Water, *Arab. J. Sci. Eng.* **41** (2016) 4775–4785.

31. Z. Li, X. Tang, K. Liu, J. Huang, Q. Peng, M. Ao and Z. Huang, Fabrication of novel sandwich nanocomposite as an efficient and regenerable adsorbent for methylene blue and Pb (II) ion removal, *J. Environ. Manage.* **218** (2018) 363–373.

32. M. R. R. Kooh, M. K. Dahri and L. B. L. Lim, The removal of rhodamine B dye from aqueous solution using Casuarina equisetifolia needles as adsorbent, *Cogent Environ. Sci.* **2** (2016) 1–14.

33. M. Özdemir, Ö. Durmuş, Ö. Şahin and C. Saka, Removal of methylene blue, methyl violet, rhodamine B, alizarin red, and bromocresol green dyes from aqueous solutions on activated cotton stalks, *Desalin. Water Treat.* **57** (2016) 18038–18048.

34. J. Geng, F. Gu and J. Chang, Fabrication of magnetic lignosulfonate using ultrasonic-assisted in situ synthesis for efficient removal of Cr(VI) and Rhodamine B from wastewater, *J. Hazard. Mater.* **375** (2019) 174–181.

35. M. Tuzen, A. Sarı and T. A. Saleh, Response surface optimization, kinetic and thermodynamic studies for effective removal of rhodamine B by magnetic AC/CeO2 nanocomposite, *J. Environ. Manage.* **206** (2018) 170–177.

36. Y. Tang, T. He, Y. Liu, B. Zhou, R. Yang and L. Zhu, Sorption behavior of methylene blue and rhodamine B mixed dyes onto chitosan graft poly (acrylic acid-co-2-acrylamide-2-methyl propane sulfonic acid) hydrogel, *Adv. Polym. Technol.* **37** (2018) 2568–2578.

37. S. S. Shenvi, A. M. Isloor, A. F. Ismail, S. J. Shilton and A. Al Ahmed, Humic Acid Based Biopolymeric Membrane for Effective Removal of Methylene Blue and Rhodamine B, *Ind. Eng. Chem. Res.* **54** (2015) 4965–4975.

38. K. Soleimani, A. D. D. Tehrani and M. Adeli, Bioconjugated graphene oxide hydrogel as an effective adsorbent for cationic dyes removal, *Ecotoxicol. Environ. Saf.* **147** (2018) 34–42.